Journal of Fluorescence (2022) 32:1959–1967
https://doi.org/10.1007/s10895-022-02992-5

ORIGINAL ARTICLE

Rapid and Highly Sensitive Detection of Target DNA Related to COVID-19 Virus With a Fluorescent Bio-conjugated Probe via a FRET Mechanism

Ghasem Rezanejade Bardajee[1] · Mohammadreza Zamani[2] · Mahdieh Sharifi[1] · Habib Rezanejad[3] · Mostafa Motallebi[2]

Received: 15 December 2021 / Accepted: 31 May 2022 / Published online: 4 July 2022

Abstract

A novel cyanine 3 (Cy3)-based bio-conjugated sensor has been developed to detect target DNA or extracted RNA from COVID -19 samples using the fluorescence resonance energy transfer (FRET) experiment. A special sequence of the COVID -19 genome was selected as a complementary DNA (target DNA) part. The opposite chain of this target sequence was designed in 2 parts; one part was attached to the Cy3 organic dye (capture DNA or Cy3- DNA), and the other part was attached to the BHQ_2 molecule (quencher DNA or BHQ_2- DNA). The Cy3 molecule acts as a donor pair, and BHQ_2 acts as an acceptor pair in the FRET experiment. The capture DNA and quencher DNA can form a sandwiched complex in the presence of target DNA. The formation of the entitled sandwiched hybrid causes the decrement of emission intensity of the Cy3 donor in bio-conjugated Cy3-DNA via energy transfer from Cy3 (as a donor) to BHQ_2 (as an acceptor). Indeed, in the presence of non-complementary DNA, the pairing of DNA strands does not occur, the FRET phenomenon does not exist, and therefore fluorescence intensity of Cy3 does not decrease. Moreover, this biosensor was successfully applied to analyze real samples containing extracted RNA of COVID -19 prepared for the reverse transcriptase-polymerase chain reaction (RT-PCR) test, and the results were promising.

Keywords Bio-conjugated sensor · Organic dyes · COVID -19 Virus · Complementary DNA · Fluorescence resonance energy transfer

Introduction

Fluorescence resonance energy transfer (FRET) has been widely used as a spectroscopic method in different applications such as medical diagnostics, DNA analysis, optical imaging, and sensing [1–4]. The attractive features promote a simple and sensitive approach for DNA detection [5] and low cost for human virus detection [6]. For a highly sensitive and rapid application of FRET-based sensors, the labels of hybridization probes and the number of targets to be detected are important [7]. FRET contains an excited donor and an acceptor, and the efficiency of the FRET system is significantly dependent on the acceptor type [5, 8]. Organic dyes are one kind of the common fluorescence materials used widely in FRET experiments. These compounds can conjugate to various substrates, such as proteins and nucleic acids, and because of this, they have a wide range of biological applications. Besides, recent advances in producing photostable dyes with high quantum yields have increased the number of applications [9]. In general, organic dyes have recently attracted much attention in several fields, such as cell imaging, molecular diagnosis, dynamic monitoring (even in vivo imaging), and human virus detection [10, 11]. One of the most common organic dyes is cyanine dyes, such as cyanine 3 (Cy3) and Cy5, which are highly regarded in medical applications and biological research [12, 13]. They have

✉ Ghasem Rezanejade Bardajee
rezanejad@pnu.ac.ir; ghrezanejad@yahoo.com

[1] Department of Chemistry, Payame Noor University, Tehran, PO BOX 19395-3697, Iran

[2] Department of Plant Biotechnology, National Institute for Genetic Engineering and Biotechnology (NIGEB), Tehran 14155-6343, PO BOX, Iran

[3] Department of Biological Sciences, MacEwan University, Edmonton, Canada

two nitrogen-containing heterocyclic rings connected via a conjugated olefin chain (Fig. 1a). Heterocyclic groups at both ends of the chain are essential for the compound to be stable [14]. Cy3 and Cy5 derivatives have been investigated as fluorophores to detect microRNA (miRNA) in a novel switch-conversion ratiometric fluorescence biosensor. This probe has been developed to overcome the low detection performance and selectivity of previous ratiometric fluorescence biosensors [15]. Cy3-conjugated gold nanoparticles (AuNPs) have been used for the detection of chloramphenicol (CAP), in which Cy3 molecules functioned as energy donors and AuNPs as energy acceptors [16]. Moreover, the detection of multiple miRNAs has been investigated by DNA tetrahedron nanotags and FRET from one nucleic acid stain TOTO-1, including Cy3, Cy3.5, and Cy5 [17].

In December 2019, an acute respiratory viral disease was transmitted to humans by a virus called coronavirus disease of 2019 (COVID -19), which originated in Wuhan, Hubei Province, China. The disease spread rapidly throughout the world and caused an increase in mortality among humans, especially in the elderly [18, 19]. Coronaviruses are members of the Coronaviridae family consists of four genera: Alphacoronavirus, Betacoronavirus, Gammacoronavirus, and Deltacoronavirus. Coronaviruses (27–32 kb) are single-stranded, positive-sense RNA

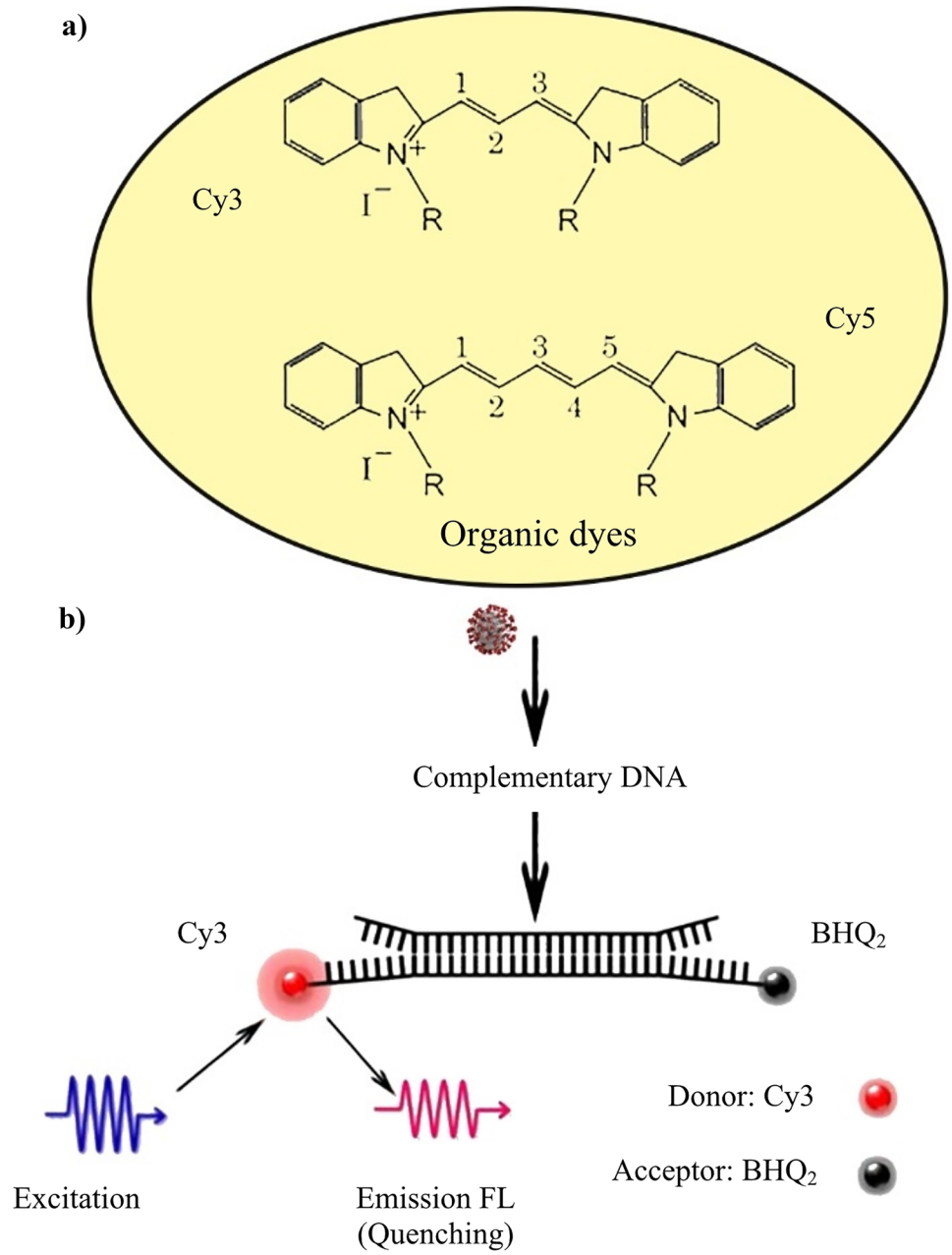

Fig. 1 **a**) Chemical structure of Cy3 and Cy5 organic dyes. **b**) The proposed performance of the Cy3-based biosensor for the detection of complementary DNA

viruses, and their genomes are among the largest of all RNA viruses. Nucleocapsid protein (N) forms the capsid outside the genome. The genome is further backed by an envelope composed of membrane protein (M), spike protein (S), and envelope protein (E) [20]. The genome size of SARS-CoV-2, which was sequenced in 2020, is approximately 29.9 kb [21]. The S glycoprotein plays an essential role in the virus attachment, fusion, and entry in to host cells. Hence, the surface localization of the S glycoprotein makes it a direct target for host immune responses, making it a prime target for neutralizing antibodies. Given its important roles in viral infection and adaptive immunity, protein S is at the heart of most vaccine strategies and therapeutic interventions [22–24]. Different variants of this SARS-CoV-2 respiratory virus (COVID-19) mainly affect the lungs, but it also has the potential to infect other vital organs, such as the heart, kidneys, and brain [25, 26].

To deal with this viral catastrophe, the first step is to quickly identify the suspect person to avoid the broad spread of the virus [27, 28]. The reverse transcription-polymerase chain response (RT-PCR) test is the foremost routinely utilized strategy to identify SARS-CoV-2 contaminations. Although this technique seems good, other methods need to be introduced to deal with this pandemic. Of course, it should be noted that there are many false negatives in the former method leading to inaccurate results. The false-negative results can be reached because of sample degradation, quality of sample collection, and the low efficiency of some test kits [27]. The present study aimed to introduce a novel Cy3-based biosensor for rapid and sensitive detection of target DNA or extracted RNA from COVID -19 samples using FRET experiment (Fig. 1b). In this regard, a simple, highly sensitive, selective, and quick approach is introduced to sense complementary DNA structure from a definite part of the COVID-19 virus genome with a good detection limit based on the FRET experiment. In addition, the intended sensor was well applied for the detection of RNA from COVID-19 viruses in clinical real samples from the upper respiratory tract with reasonable analytical outcomes, and the results are compared with RT-PCR as the established standard system. In the existence of the target fragment, a "sandwich" hybrid assembly is formed that decreases the fluorescence intensity of the Cy3 dye via transferring energy from the excited state of the dye to the quencher molecule through the FRET mechanism. The results showed that positive samples with lower fluorescence levels corresponded to those with low Ct values in RT-PCR, suggesting a correlation between viral load and fluorescence decrement. However, the entitled system is mainly based on fluorescence spectroscopy, and its acceptable performance opens a new window in COVID-19 detection research.

Experimental

Chemicals and Reagents

Tris–HCl was purchased from Carloerba Reagents. NaCl, $MgCl_2$, and NaOH were prepared from Merck. The RNase-free water and RNA of COVID -19 were provided by National Institute for Genetic Engineering and Biotechnology (NIGEB), Iran. Double distilled water (DDW) with high purity was used during the whole analysis process. DNA oligonucleotides were chemically synthesized by Metabion (Germany) with the following sequences:

Capture DNA (Cy3- DNA): 5′-Cy3–GTACTGTAGGC-3′ (11-mer)
Quencher DNA (BHQ_2- DNA): 5′-CGGCACTTGTG-BHQ_2-3′ (11-mer)
Complementary DNA (target DNA): 5′-CACAAGTGC CGGCCTACAGTAC-3′ (22-mer: This arrangement has been planned based on a specific sequence of the COVID -19 genome)
Non- complementary DNA (non-target DNA): 5′-GTG ACATGACATCCGTTCGTGA -3′ (22-mer)

Preparation of DNA Stock Solutions and Tris Buffer

DNA stock solutions with a concentration of 100 µM were prepared by adding 162, 216, 198, and 265 µL of RNase-free water to capture DNA, quencher DNA, complementary DNA, and non- complementary DNA, respectively, and stored at -4 ˚C.

The Tris buffer containing 960 mM Tris–HCl, 0.1 M NaCl, and 10 mM $MgCl_2$ was prepared, and the pH was adjusted to 7.6 by adding 0.1 M NaOH.

Fluorescence and Absorption Spectra emission spectra were obtained with a Shimadzu RF-6000 spectrofluorometer (Japan) and scanned in 540–700 nm at the excitation wavelength of 520 nm. The slit width for excitation and emission were 5 nm, respectively. The UV–Vis absorption spectra of samples were collected using a Shimadzu UV–Vis spectrophotometer (Japan) with wavelength of 200–700.

Detection of Target Complementary DNA

The assay procedure for the detection of complementary DNA was as follows: In a sterilized vial, 20 µL of capture DNA (Cy3-DNA [0.6 µM]) was mixed with 120 µL of RNase-free water (or buffer solution). Then, 20 µL quencher DNA (0.6 µM) and 20 µL complementary DNA (0.6 µM)

were added to the above solution and mixed for the appropriate time. Finally, the solution was transferred to a quartz micro-cuvette, and the corresponding spectra were taken at an excitation wavelength of Cy3 (520 nm). The same procedure was applied for the non- complementary DNA assay.

Optimization of Conditions

To investigate the effect of solvent on the efficiency of the detection system, a series of solutions containing complementary DNA or non-complementary DNA molecules with different concentrations (0.003 µM, 0.01 µM, 0.02 µM, 0.04 µM, 0.07 µM, and 0.19 µM) were prepared in both RNase-free water and Tris buffer media. Then the fluorescence spectra were collected, respectively.

The effects of interaction times and temperature on the fluorescence emission intensity of samples containing complementary and non- complementary were also investigated. The fluorescence spectra were collected when complementary or non- complementary (with a final concentration of 0.06 µM) was added to the detection system, and the reaction time ranged from 5 to 60 min (5, 10, 15, 20, 30, 40, 50, and 60 min) at room temperature. Besides, the same system was applied to optimize temperatures of about 5, 25, 40, and 60 °C within 20 min.

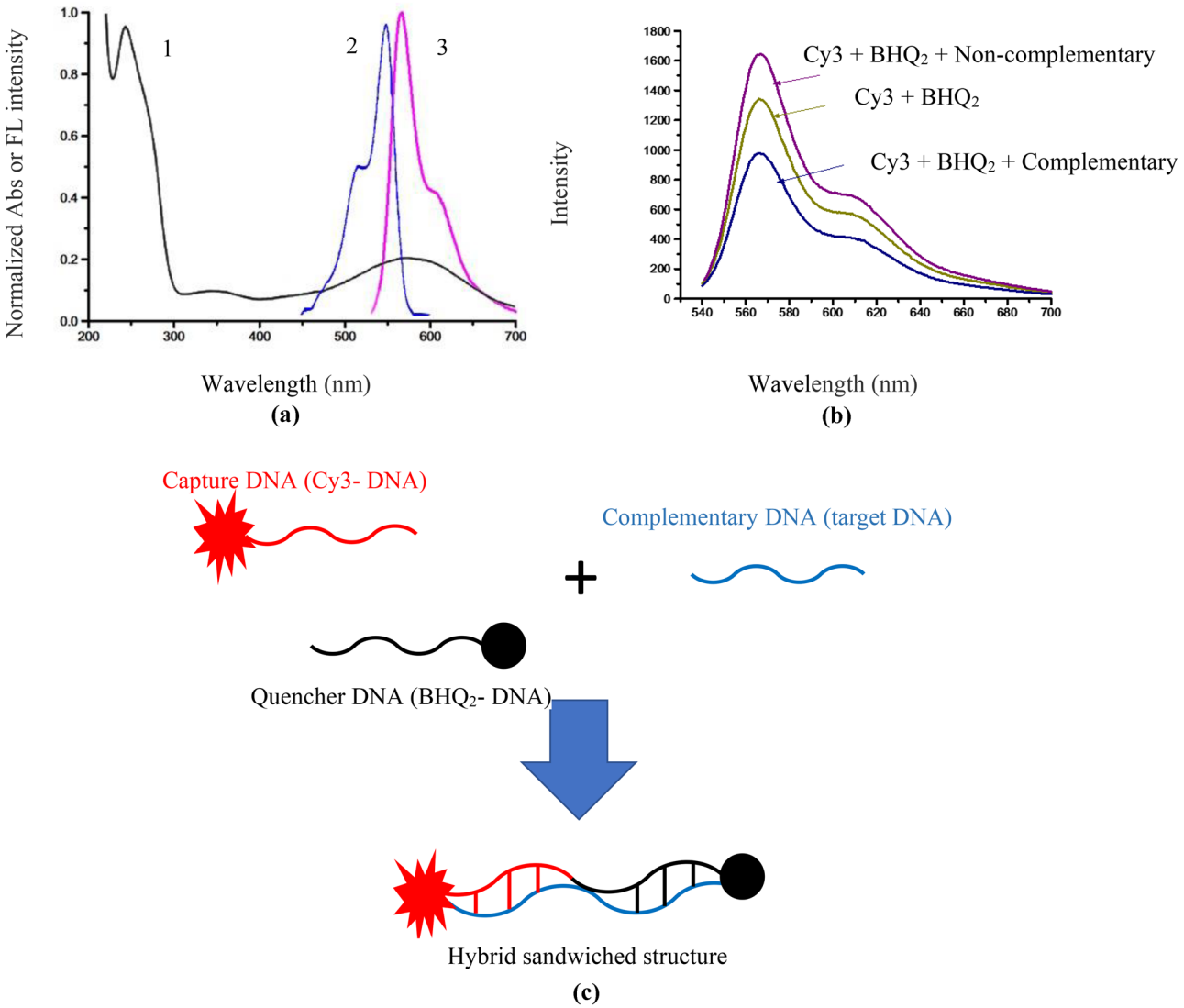

Fig. 2 **a**) Normalized absorption and fluorescence spectra of BHQ_2 and Cy3 (1 [black]: absorption spectrum of BHQ_2; 2 [blue]: absorption spectrum of Cy3; and 3 [pink]: fluorescence spectrum of Cy3). **b**) FL spectra of Cy3-DNA + BHQ_2- DNA mixed solutions, sandwiched hybrid system (Cy3-DNA + BHQ_2-DNA + complementary DNA), and non-hybrid system (Cy3-DNA + BHQ_2-DNA + non-complementary DNA) with same concentrations in RNase-free water. **c**) A schematic representation for pairing different DNA single strands (containing Cy3-DNA, BHQ_2-DNA, and complementary DNA) to form a hybrid sandwiched structure

Real Sample Analysis

The extracted RNA samples from the saliva of COVID -19 suspects were analyzed by the developed method. The samples containing RNA of positive COVID -19 or without it (negative COVID-19) were diluted with ten µL RNase-free water. They were added to the detection system containing a Cy3-DNA probe and quencher DNA in an RNase-free water medium. The fluorescence spectra were collected after incubation for 20 min, respectively.

Results and Discussion

Optical Properties

UV–Vis spectra of quencher DNA (BHQ_2-DNA), the absorption spectrum of Cy3, and fluorescence spectra of Cy3 are shown in Fig. 2a. As can be seen, the maximum absorption peak of BHQ_2-DNA is 573 nm. While a shoulder was recognized in the absorption spectrum, Cy3 shows maxima at 550 nm and 566 nm for the absorption and fluorescence

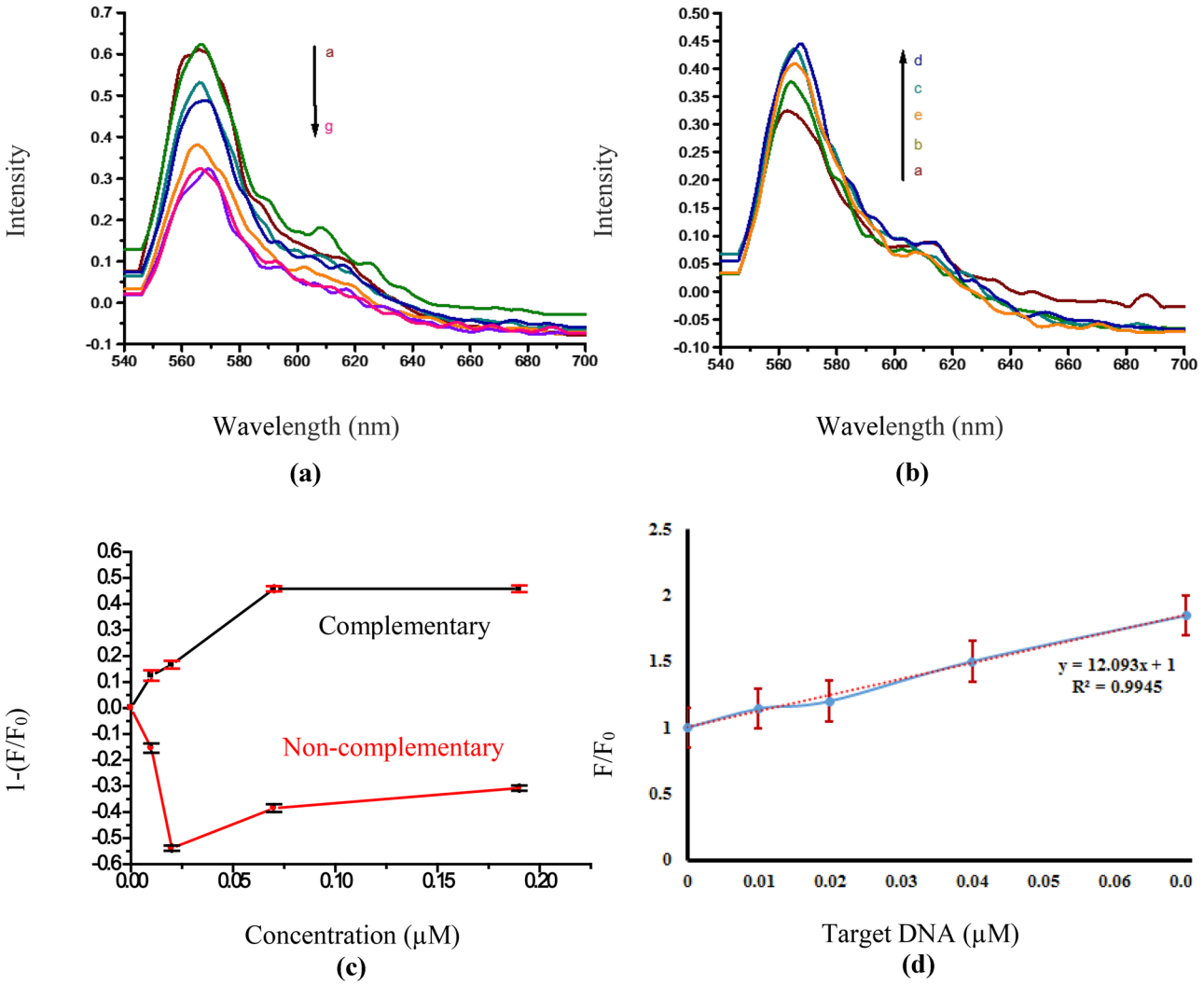

Fig. 3 **a**) Emission spectra of the biosensor containing different concentrations of complementary DNA in RNase-free water (a→g: 0 µM, 0.003 µM, 0.01 µM, 0.02 µM, 0.04 µM, 0.07 µM, 0.19 µM). **b**) Emission spectra of the biosensor containing different concentrations of non-complementary DNA in RNase-free water (a→e: 0 µM, 0.01 µM, 0.02 µM, 0.07 µM, 0.19 µM). **c**) The different quenching behavior of the hybrid and non-hybrid systems for better distinguishing the target from the non-target DNA molecule in RNase-free water. **d**) The plot for the fluorescence quenching fraction (at λ 566 nm) of the probe versus the concentrations of target DNA

spectra. Furthermore, the fluorescence spectra of Cy3-BHQ2 mixed solutions, sandwiched hybrid system (containing Cy3-DNA, BHQ_2-DNA, and complementary DNA), and non-hybrid system (including Cy3-DNA, BHQ_2-DNA, and non-complementary DNA) with same concentrations in RNase-free water are shown in Fig. 2b. As expected, the fluorescence intensity of the reference sample (containing mixed Cy3-DNA and BHQ_2-DNA solutions) was gradually decreased by adding complementary DNA with a maximum emission wavelength of 566 nm. However, the fluorescence intensity of the reference sample was slightly increased by adding non-complementary DNA at the same maximum emission wavelength. Indeed, the Cy3-DNA bio-conjugated chains and the BHQ_2-DNA oligonucleotides were paired with the single-stranded target complementary DNA to form a hybrid sandwiched structure (Fig. 2c). As a result of this pairing (sandwiched form), the Cy3 donor molecules and the BHQ_2 acceptor molecules were placed at a reasonable distance to transfer energy through FRET, resulting in a reduction in the fluorescence intensity of the molecule (Fig. 1b). However, in the presence of presence of the non-complementary DNA (non-target DNA), this pairing did not occur (no sandwiched form). As a result, there was no energy transfer through FRET; hence, the emission intensity of the Cy3 donor molecule did not decrease.

Detection Ability in RNase-free Water and Buffer Media

The difference between RNase-free water and Tris buffer as a solvent in the detection efficacy is depicted in Figs. 3 and

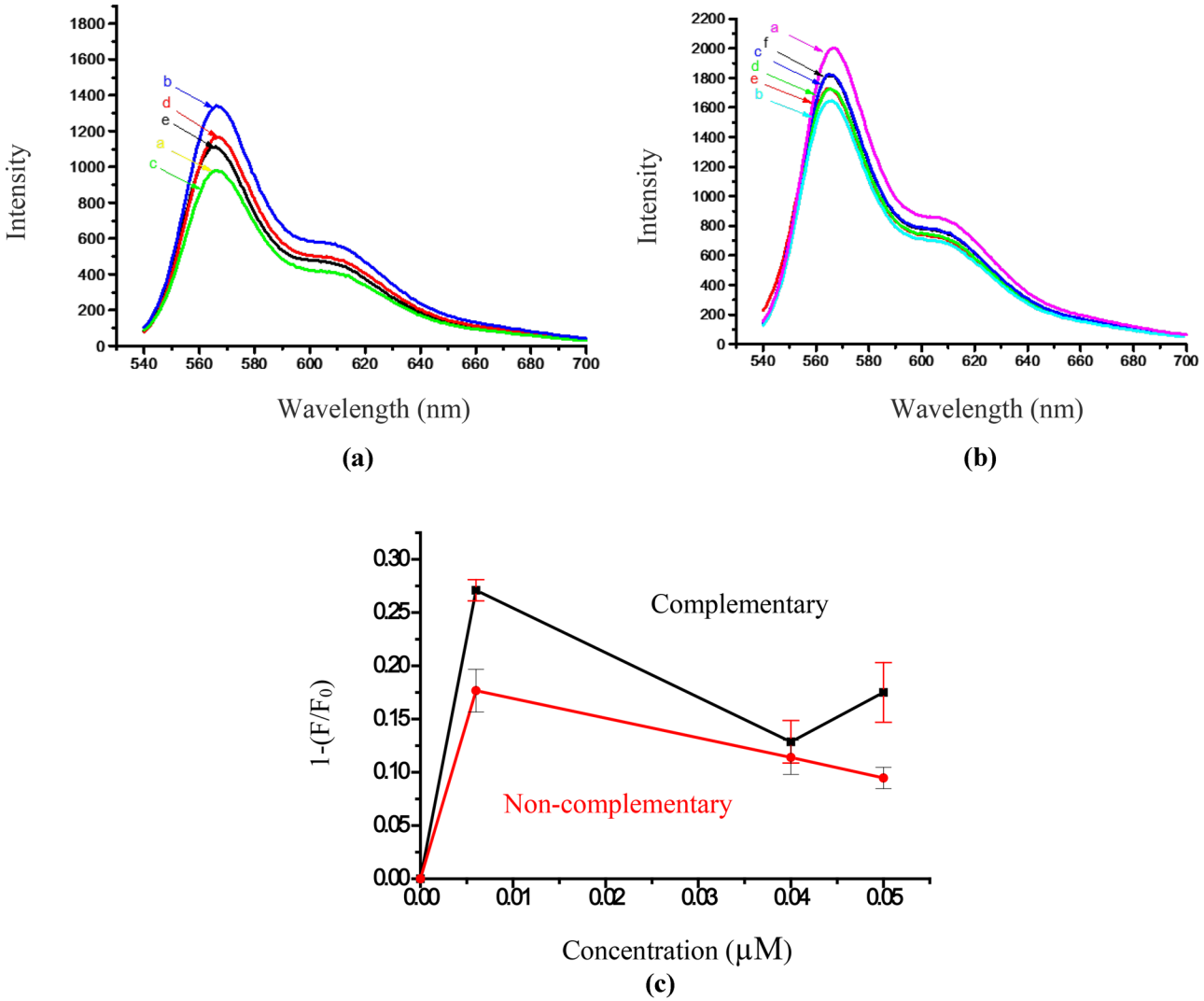

Fig. 4 **a**) Emission spectra of the biosensor containing different concentrations of complementary DNA in Tris buffer (a→f: 0 μM, 0.006 μM, 0.04 μM, 0.05 μM). **b**) Emission spectra of the biosensor containing different concentrations of non-complementary DNA in Tris buffer (a→f: 0 μM, 0.006 μM, 0.04 μM, 0.05 μM). **c**) Dose–response curve for complementary DNA and non-complementary DNA samples at different concentrations in Tris buffer

4, respectively. From the emission spectra (Fig. 3a), it can be seen that the fluorescence intensities for the hybrid system containing Cy3 nanoprobe, quencher DNA, and complementary DNA were gradually decreased by increasing the concentration of complementary (target DNA) from 0.003 µM to 0.019 µM in RNase-free water. In contrast, the diminution of the intensity was minor, with further increasing the concentration of the complementary oligonucleotide. The addition of non-target DNA in RNase-free water (Cy3 nanoprobe, quencher DNA, and non-complementary DNA) was also investigated. As shown in Fig. 3b, the fluorescence intensity of the band at 564 nm was enhanced slightly by increasing the concentrations of non-complementary DNA from 0.01 µM to 0.019 µM. Indeed, these results confirm that in the presence of non- complementary DNA, the pairing of DNA strands does not occur, the FRET phenomenon does not exist, and therefore fluorescence intensity of Cy3 does not decrease. As shown in Fig. 3c, the quenching value (Y-axis) of Cy3 increases with increasing the concentration of complementary (target DNA). At the same time, it slightly decreases with increasing the concentrations of non-complementary DNA in RNase-free water, resulting in a typical different quenching behavior curve of the hybrid and non-hybrid systems.

Moreover, the curve for the fluorescence quenching fraction of the probe versus the concentration of complementary DNA presented satisfactory linearity in the concentration of complementary DNA, ranging from 0 µM to 0.07 µM (Fig. 3d). The linear regression equation was $y = 12.093x + 1$ with a regression coefficient of 0.09945, indicating that the Cy3 probe can be used with confidence to determine the complementary DNA concentration in low concentrations. The limit of detection (LOD) for the probe was evaluated using 3 s/S and was found to be 0.0995 µM, where s is the standard deviation of the blank signal, and S is the slope of the linear calibration plot. The limit of quantity (LOQ) for the probe was evaluated using 10 s/S and was reported 0.3316 µM.

Similar experiments were performed in the Tris buffer medium. Due to the higher detection efficiency of RNase-free water than the tris buffer, RNase-free water was selected as the optimum medium for the hybrid detection system (Fig. 4). The lower efficiency of the hybrid system in the Tris buffer could be related to the interfering effect of different ions in the buffer to prevent DNA strands from pairing.

The Effect of Interaction Time and Temperature on Detection Efficacy

The fluorescence intensity of the biosensor with fixed concentration levels of complementary DNA (20 µL, 0.05 µM) in various interaction times ranging from 5 to 60 min was examined in RNase-free water. As can be seen in Fig. 5a, when the concentration of both the Cy3-DNA probe and quencher DNA was 20 µL (0.05 µM), the fluorescence intensity of the biosensor at 564 nm gradually decreased until it reached 77% quenching after 20 min. After that, the fluorescence intensity of the biosensor did not decrease anymore with further increasing the interaction time. Figure 5b shows the effects of temperature (5, 25, 40, and 60 °C) on the fluorescence emission intensity of the biosensor containing Cy3-DNA probe, quencher DNA, and complementary DNA with the same concentrations in RNase-free water. It is clear that the fluorescence intensities of the probe were mostly similar to each other at room temperature and 40 °C and increased at 5 and 60 °C. However, the room temperature (25 °C) and 20 min of incubation were fixed for all tests as optimum conditions for further experiments.

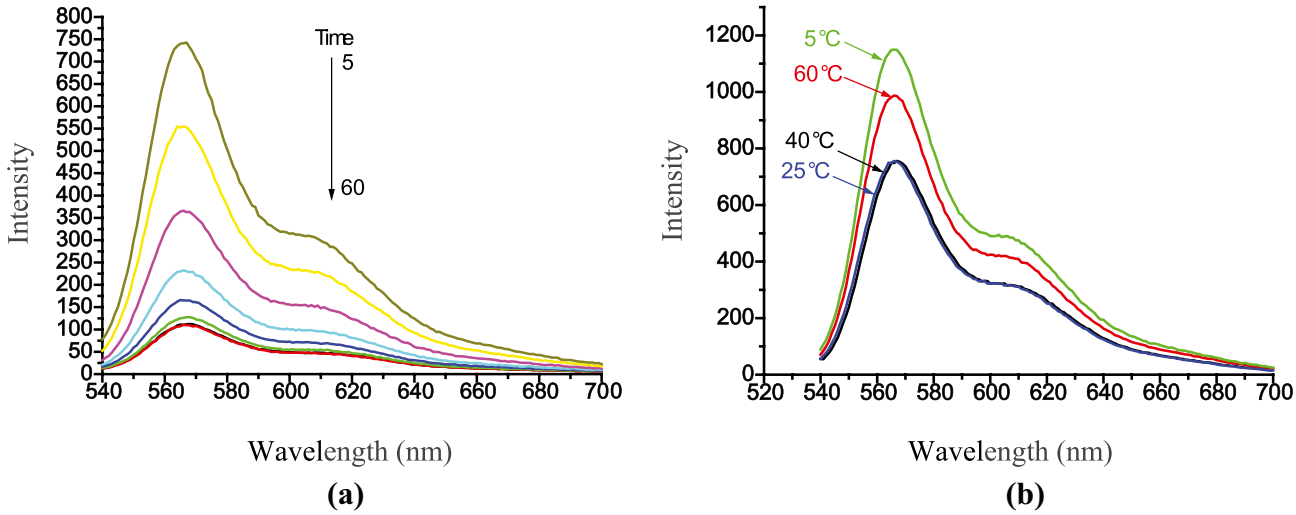

Fig. 5 **a**) The interaction time from 0 to 60 min on the responses of the fluorescent biosensor in RNase-free water. **b**) The effects of temperature (5, 25, 40, and 60 °C) on the FL intensity of the biosensor

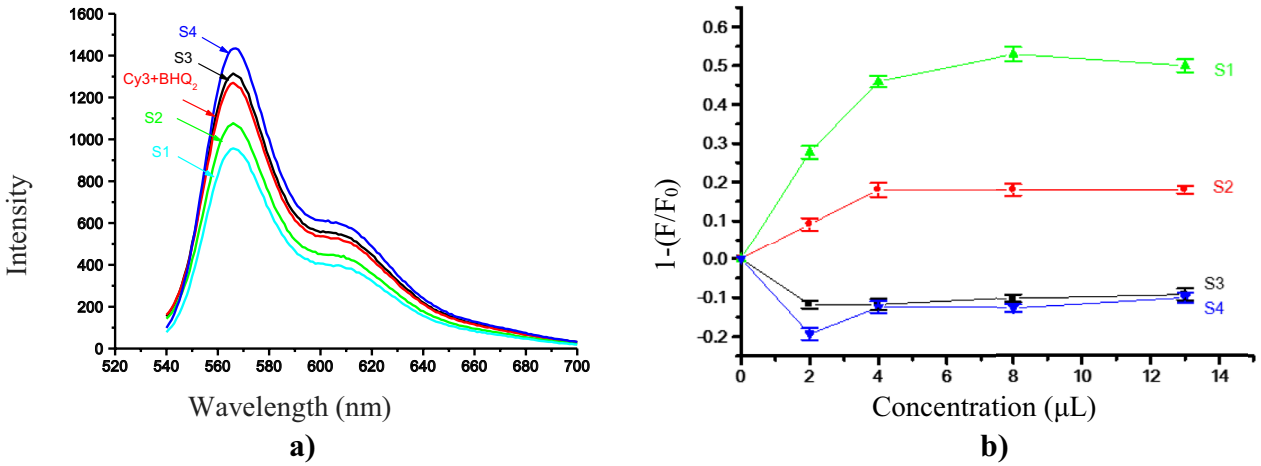

Fig. 6 **a**) FL spectra of the biosensor containing the target molecule (S1 and S2: with RNA of COVID -19) and non-target molecule (S3 and S4: without RNA of COVID -19) in the real samples. **b**) Dose–response curve for samples S1-S4 (S1-S2 = positive and S3-S4 = negative) in different concentrations to highlight the ability of the proposed system for detecting the virus in real samples

Analysis of Real Samples Containing Extracted RNA of COVID -19 from the Saliva of COVID-19 Suspects

Based on the above results, the entitled biosensor was applied for the analysis of 2 positive (S1 and S2: containing RNA of COVID -19) and 2 negative (S3 and S4: without RNA of COVID -19) samples received from the National Institute for Genetic Engineering and Biotechnology (Iran). These samples were collected from the saliva of individuals suspected of COVID -19 after extracting their RNA. According to Fig. 6a, the fluorescence intensities of positive samples constructing the sandwiched hybrid system (containing Cy3-DNA probe, quencher DNA, and RNA of COVID -19 as target molecules) significantly decreased compared to the reference probe (mixed Cy3-DNA probe and quencher DNA) in RNase-free water solvent. However, the fluorescence intensities of the negative samples without RNA of COVID -19 (non-hybrid system) slightly increased compared to the reference probe in RNase-free water. As expected, the entitled biosensor displayed excellent performance for RNA of COVID -19 detection, which was in good agreement with the results of the standard RT-PCR method. The difference between positive and negative samples is shown very clearly by the dose–response curve in Fig. 6b.

Conclusions

A novel fluorescent biosensor based on a Cy3 organic dye was applied for rapid and sensitive detection of target complementary DNA or extracted RNA from COVID -19 based on the FRET experiment. In this system, a Cy3-DNA bio-conjugated probe (as a donor) and BHQ_2-DNA (as an acceptor; quencher) were coupled to work well in the FRET mechanism. Indeed, in the presence of the target DNA or RNA from COVID -19, a sandwiched hybrid structure was developed, affecting the fluorescence intensity of the donor molecule. Besides, the fluorescence quenching values of the probe versus the concentration of complementary DNA presented excellent linearity leading to the satisfactory LOD of 0.0995 μM and LOQ of 0.3316 μM. Furthermore, this biosensor showed good potential for the analysis of real samples containing extracted RNA of COVID -19 with an excellent ability to distinguish between positive and negative samples. Since the developed method is rapid and sensitive, this work provides new clues for further research to replace the expensive RT-PCR method with fluorescence probes for the detection of COVID -19.

Authors' Contribution Ghasem Rezanejade Bardajee and Mohammadreza Zamani conceptualized the research topic. Mahdieh Sharifi prepared the research proposal and did the main part of the experiments. Ghasem Rezanejade Bardajee, Mohammadreza Zamani, and Mahdieh Sharifi interpreted the results and prepared the draft. Habib Rezanejad and Mostafa Motallebi contributed in revised manuscript.

Funding The authors are grateful to NIGEB for their financial support of this work.

Data Availability Not applicable.

Code Availability Not applicable.

Declarations

Ethics Approval The submitted work is original and not published elsewhere. This manuscript is presented clearly and not split up into several

parts to increase the quantity of submissions. All authors are adhered to discipline-specific rules for acquiring, selecting, and processing data. We acknowledged other works properly in a suitable position.

Consent to Participate All the authors were aware of the submission and agreed to its publication.

Consent for Publication We wish to inform you that the data and ideas presented in the manuscript are of our own and are not under consideration for publication elsewhere.

Conflicts of Interest The authors declare that they have no known competing financial interests or personal relationships that could have appeared to influence the work reported in this paper.

References

1. Chen G, Song F, Xiong X, Peng X (2013) Fluorescent nanosensors based on fluorescence resonance energy transfer (FRET). Indust Eng Chem Res 52(33):11228–11245
2. Kwon L, Long K, Wan Y, Yu H, Cunningham B (2016) Medical diagnostics with mobile devices: Comparison of intrinsic and extrinsic sensing. Biotechnol Adv 34(3):291–304
3. Ho F-C, Huang K-H, Cheng H-W, Huang Y-J, Nhien PQ, Wu C-H, Wu JI, Chen S-Y, Lin H-C (2021) FRET processes of bifluorophoric sensor material containing tetraphenylethylene donor and optical-switchable merocyanine acceptor for lead ion ($Pb2^{+}$) detection in semi-aqueous media. Dyes Pigm 189:109238
4. Bardajee GR, Zamani M, Sharifi M (2021) Efficient and Versatile Application of Fluorescence DNA-Conjugated CdTe Quantum Dots Nanoprobe for Detection of a Specific Target DNA of SARS Cov-2 Virus. Langmuir 37(33):10223–10232
5. Tian J, Zhao H, Liu M, Chen Y, Quan X (2012) Detection of influenza A virus based on fluorescence resonance energy transfer from quantum dots to carbon nanotubes. Anal Chim Acta 723:83–87
6. Shamsipur M, Nasirian V, Mansouri K, Barati A, Veisi-Raygani A, Kashanian S (2017) A highly sensitive quantum dots-DNA nanobiosensor based on fluorescence resonance energy transfer for rapid detection of nanomolar amounts of human papillomavirus 18. J Pharmaceut Biomed Anal 136:140–147
7. Marras SA (2006) Selection of fluorophore and quencher pairs for fluorescent nucleic acid hybridization probes. Fluorescent Energy Trans Nucleic Acid Probes 3–16
8. Dong L-Y, Wang L-Y, Wang X-F, Liu Y, Liu H-L, Xie M-X (2016) Development of fluorescent FRET probe for determination of glucose based on β-cyclodextrin modified ZnS-quantum dots and natural pigment 3-hydroxyflavone. Dyes Pigments 128:170–178
9. Kaur A, Dhakal S (2020) Recent applications of FRET-based multiplexed techniques. Trends Anal Chem 123:115777
10. Quan K, Yi C, Yang X, He X, Huang J, Wang K (2020) FRET-based nucleic acid probes: Basic designs and applications in bioimaging. TrAC, Trends Anal Chem 124:115784
11. Jia F, Diao P, Wang X, Hu X, Kimura T, Nakamuta M, Nakamura I, Shirotori S, Sato Y, Moriya K (2020) Dietary Restriction Suppresses Steatosis-Associated Hepatic Tumorigenesis in Hepatitis C Virus Core Gene Transgenic Mice. Liver cancer 9(5):529–548
12. Liu H, Yin J, Xing E, Du Y, Su Y, Feng Y, Meng S (2021) Halogenated Cyanine Dyes for Synergistic Photodynamic and Photothermal Therapy. Dyes and Pigm 109327
13. Shindy H (2017) Fundamentals in the chemistry of cyanine dyes: A review. Dyes Pigm 145:505–513
14. Wang L, Xiang J, Sun H, Yang Q, Yu L, Li Q, Guan A, Tang Y (2015) Controllable cy3-MTC-dye aggregates and its applications served as a chemosensor. Dyes Pigm 122:382–388
15. Chen X, Xu K, Li J, Yang M, Li X, Chen Q, Lu C, Yang H (2020) Switch-conversional ratiometric fluorescence biosensor for miRNA detection. Biosens Bioelectron 155:112104
16. Zhang Y, Li C-W, Zhou L, Chen Z, Yi C (2020) "Plug and Play" logic gate construction based on chemically triggered fluorescence switching of gold nanoparticles conjugated with Cy3-tagged aptamer. Microchim Acta 187(8):437
17. Zhao H, Wang M, Xiong X, Liu Y, Chen XJT (2020) Simultaneous fluorescent detection of multiplexed miRNA of liver cancer based on DNA tetrahedron nanotags 210:120677
18. Yuki K, Fujiogi M, Koutsogiannaki SJCi (2020) COVID-19 pathophysiology: A review. Clinic Immunol 108427
19. Liu S, Yang L, Zhang C, Xiang Y-T, Liu Z, Hu S, Zhang B (2020) Online mental health services in China during the COVID-19 outbreak. The Lancet Psych 7(4):e17–e18
20. Brian D, Baric R (2005) Coronavirus genome structure and replication. Coronavirus replication reverse genetics1–30
21. Lu R, Zhao X, Li J, Niu P, Yang B, Wu H, Wang W, Song H, Huang B, Zhu N (2020) Genomic characterisation and epidemiology of 2019 novel coronavirus: implications for virus origins and receptor binding. The lancet 395(10224):565–574
22. Vardhan S, Sahoo SK (2022) Virtual screening by targeting proteolytic sites of furin and TMPRSS2 to propose potential compounds obstructing the entry of SARS-CoV-2 virus into human host cells. J Tradition Complement Med 12(1):6–15
23. Vardhan S, Sahoo SK (2022) Exploring the therapeutic nature of limonoids and triterpenoids against SARS-CoV-2 by targeting nsp13, nsp14, and nsp15 through molecular docking and dynamics simulations. J Tradition Complement Med 12(1):44–54
24. Vardhan S, Sahoo SK (2020) In silico ADMET and molecular docking study on searching potential inhibitors from limonoids and triterpenoids for COVID-19. Comput Biol Med 124:103936
25. Vardhan S, Sahoo SK (2022) Computational studies on the interaction of SARS-CoV-2 Omicron SGp RBD with human receptor ACE2, limonin and glycyrrhizic acid. Comput Biol Med 144:105367
26. Pal M, Berhanu G, Desalegn C, Kandi V (2020) Severe acute respiratory syndrome coronavirus-2 (SARS-CoV-2): an update. Cureus 12 (3)
27. Sheikhzadeh E, Eissa S, Ismail A, Zourob M (2020) Diagnostic techniques for COVID-19 and new developments. Talanta:121392
28. Haleem A, Javaid M, Khan IH, Vaishya R (2020) Significant applications of big data in COVID-19 pandemic. Indian J Ortho 54:526–528